GeoPlanning
Journal of Geomatics and Planning
Vol. 8, No. 1, 2021

e-ISSN: 2355-6544

Received: 1 January 2020;
Accepted: 1 January 2021;
Published: 30 July 2021.

Keywords:
NCEP, GNSS, Water Vapour, NigNet, Rainfall

*Corresponding author(s) email:
bswafiyudeen@gmail.com

Original Research Open access

Modelling Precipitable Water Vapour (PWV) Over Nigeria from Ground-Based GNSS

Bawa Swafiyudeen [1*], Usman I. Sa'i [1], Adamu Bala [1], Aliyu Z. Abubakar [1], Adamu A. Musa [2], Nura Shehu [1]

1. *Department of Geomatics, Ahmadu Bello University, Zaria, Kaduna, Nigeria*
2. *Department of Surveying and Geoinformatics, Nuhu Bammalli Poly, Zaria, Kaduna, Nigeria*

DOI: 10.14710/geoplanning.8.1.41-50

Abstract

Global Navigational Satellite System (GNSS) over the past and present time has shown a great potential in the retrieval of the distribution of water vapour in the atmosphere. Taking the advantage of the effect of the atmosphere on GNSS signal as they travel from the constellation of satellite to ground-based GNSS receivers such that information (water vapour content) about the atmosphere (mostly from the troposphere) can be derived is referred to as GNSS meteorology. This paper presents the spatiotemporal variability of Precipitable Water Vapour (PWV) retrieved from ground–based Global Navigation Satellite System (GNSS) stations over Nigeria for the years 2012 to 2013. In this paper, the GNSS data were processed using GAMIT (ver. 10.70). The GNSS PWV were grouped into daily and monthly averages; the variability of the daily and monthly GNSS PWV were compared and validated with the daily and monthly PWV from National Centre for Environmental Prediction (NCEP) and monthly Rainfall data for the study years respectively. The results revealed that the spatiotemporal variability of PWV across Nigeria is a function of geographic location and seasons. The result shows that there is temporal correlation between GNSS PWV, NCEP PWV and rainfall events. The research also affirms that GNSS PWV could be used to improve weather forecasting/monitoring as well as climate monitoring.

Copyright © 2021 GJGP-Undip
This open access article is distributed under a
Creative Commons Attribution (CC-BY-NC-SA) 4.0 International license

1. Introduction

Global Navigational Satellite System (GNSS) over the past and present time has shown a great potential in the retrieval of the distribution of water vapour in the atmosphere (see for example Bevis et al., 1994, 1992; Davis et al., 1985; Gurbuz et al., 2015; Isioye et al., 2016). The potential of GNSS in meteorology was first proposed by Bevis et al. (1992). Ground-based GNSS meteorology can be advantageous in numerical weather forecasting. Regionally and globally, it can be adopted for climate monitoring and atmospheric research.

Taking the advantage of the effect of the atmosphere on GNSS signal as they travel from the constellation of satellite to ground-based GNSS receivers such that information (water vapour content) about the atmosphere (mostly from the troposphere) can be derived is referred to as GNSS meteorology (Xiaoming et al., 2010; Uang-Aree et al., 2014). Water vapour gradiometers, LiDAR, Radio Sounds and solar spectrometers are other techniques that can be used for water vapour retrieval, but one disadvantage is that they are expensive unlike their GNSS counterpart. In this study, the GAMIT (Herring et al., 2010; Li, 2021) has been used to estimate Precipitable Water Vapour over Nigeria from ground-based GNSS stations. The ionosphere and the troposphere are among the major cause of GNSS signal delay as they travel down to the earth surface from constellation of satellite. The ionospheric delay can be mitigated using dual frequency GNSS receivers and utilizing its dispersive characteristics (Tregoning et al., 1998; Wielgosz et al., 2019; Perevalova et al., 2020). To the Geodesist, the atmospheric errors are a cause for concern but for meteorological studies, the tropospheric error is useful for climate studies and other related applications.

The delay caused by the troposphere called Zenith Total Delay (ZTD) can be divided into two parts (Liu et al., 2017). The non-hydrostatic (wet) part (ZWD) which is water vapour and temperature dependent component and the hydrostatic (dry) part (ZHD) which is surface pressure dependent (Gurbuz et al., 2015; Tsidu et al., 2015; Suresh Raju et al., 2007; Boutiouta & Lahcene, 2013) . The ZHD amounts to about 90% of the ZTD.

$$ZWD + ZHD = ZTD \quad (1)$$

The path length taken by satellite signal to the receiver can be equally expressed as Equation (2).

$$ZTD = 10^{-5} \int N(s)ds \quad (2)$$

Where $N = 10^6(n-1)$ is the atmospheric refractivity, is refractive index. In practical application, the refractivity can't be computed with high precision. Therefore, ZTD is routinely obtained from ground-based GNSS station by using high precision GNSS software like GAMIT/GLOBK as used in this study.

The ZHD can be computed using surface meteorological data given in Equation (3) (Davis et al., 1985; Saastamoinen, 1972; Chen & Liu, 2015).

$$ZHD(\rho_s, \lambda, h) = \frac{\rho_s(2.2779 \pm 0.0024)}{(1 - 0.00266\ \cos(2\lambda) - 0.00028h)} \quad (3)$$

Where ρ_s is the surface pressure in mbar, λ is the latitude of antenna and h is station altitude in kilometre above the ellipsoid. This is a function of latitude.

However, ZWD is mostly inaccurately calculated due to the dispersed and unpredictable water vapour content in the atmosphere. The errors budget can reach up to several cm at the zenith. It can be calculated by subtracting ZHD from ZTD, as given in Equation (4).

$$ZWD = ZTD - ZHD \quad (4)$$

Once ZWD is estimated, PWV can be computed. PWD is roughly proportional to ZWD, given by Equation (5)

$$PWV = \prod - ZWD \quad (5)$$

$\prod$ is a proportional constant that is dimensionless. This is given by Equation (6)

$$\prod^{-1} = 10^{-6}(k_3 T_m^{-1} + k_2')R_v \rho_v \quad (6)$$

Where k_2' and k_3 are refractivity constants with values 22.1 ± 2.2(K/mb), and 373900 105± 0.012(K2/mb) respectively. R_v is gas constant for water vapour with the value 461.524 (JK-1 Kg-1) (Bevis et al., 1992).

The parameter T_m in Equation (6) is the weighted mean temperature depending on surface temperature T_s given by (Davis et al., 1985)

$$T_m = \frac{\int (e/T)dz}{\int (e/T^2)dz} \quad (7)$$

Where e is the partial pressure of water vapour and T is absolute temperature of the surface of interest. T_m can be estimated from numerical weather model or surface temperature. The most commonly used model for the computation of T_m is given by (Bevis et al., 1994)

$$T_m = a + bT_s \quad (8)$$

The coefficients *a* and *b* are season and region specific, thus, vary from season to region. Isioye et al. (2016) provided T_m for Nigeria (Equation (9)) and the West Africa region (Equation (10)). Also, Bevis et al. (1992) provided a T*m* model as expressed in Equation (11).

$$T_m = 0.5245T_s + 132.12 \quad (9)$$

$$T_m = 0.5745T_s + 116.60 \quad (10)$$

$$T_m = 0.72T_s + 70.2 \quad (11)$$

2. Methodology

2.1. Data, Processing, and Methods

Presently, fifteen (15) CORS are available across the country as presented in Figure 1 (Bawa et al., 2017), with the station in KANO excluded because of its short data span. The summary of datasets and sources adopted for the Study is presented in Table 2 (Bawa et al., 2017). GAMIT/GLOBK Version 10.7 developed at Massachusetts Institute of Technology (MIT), the Harvard-Smithsonian Centre for Astrophysics (CfA), Scripps Institution of Oceanography (SIO), and Australian National University (Herring et al., 2010; Tsai et al., 2015; Kindu, 2017; Godah et al., 2020) was used for processing the tracking stations RINEX files. It can also be used for atmospheric delays estimation, station coordinates and velocities estimation, functional or stochastic representation of post-seismic deformation, Earth orientation parameter and satellite orbits (Herring et al., 2010). The processing parameters for accurate estimation are presented in Table 1 (Bawa et al., 2017). For a better and accurate construction of the numerical weather model (NWM) the Vienna Mapping Function one (1) (VMF1) obtained from everest.mit.edu was used to interpolate hydrostatic and wet mapping function coefficients as a function of time and location. After estimation of daily zenith total delays (ZTD) by GAMIT, PWV values are computed with sh_metutil of GAMIT using the Bevis et al. (1994, 1992) T_m model.

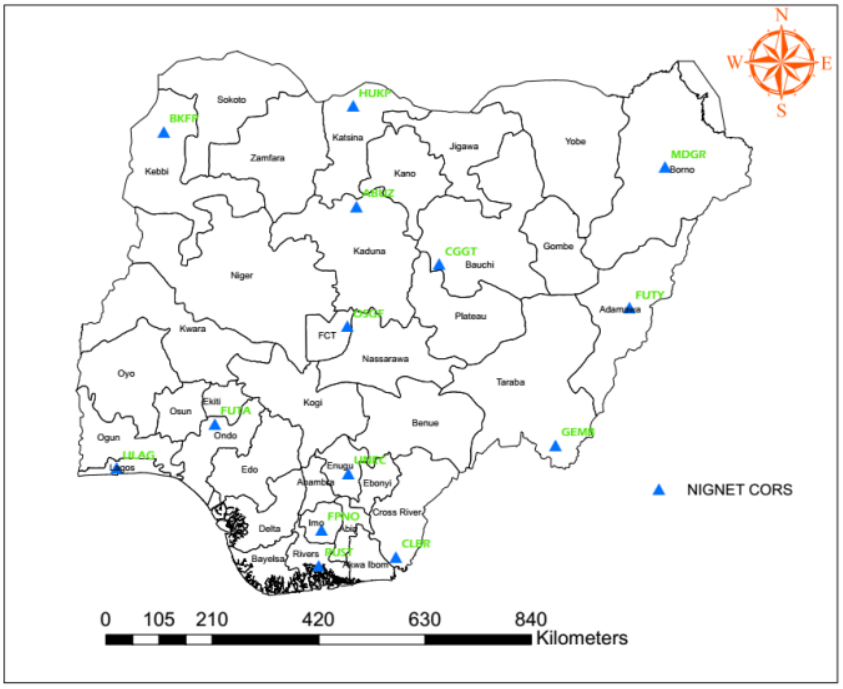

Figure 1. Spatial Distribution of CORS Stations in Nigeria

Table 1. Summary of Dataset and Sources Adopted for the Study

S/N	Dataset	Source(s)	Purpose(s)
1	RINEX files associated with 14 selected NigNet tracking stations from 1st January 2011 to 31st December 2015 (1826 days)	www.nignet.net	Time series analysis, position and velocity estimate and strain computation
2	Nine (9) International GNSS Services (IGS) sites stations from 1st January 2011 to 31st December 2015 (1826 days)	ftp://cddis.gsfc.nasa.gov	Position, velocity and Frame Realization
3	SP3 precise ephemeris orbits	http://cddis.nasa.gov	For GAMIT/GLOBK processing
4	Ocean tide loading model(FES2004)	ftp://everest.mit.edu/pub/GRIDS	Correction for Ocean tide loading
5	Dry and Wet Mapping Function (VMF1)	ftp://everest.mit.edu/pub/GRIDS	Incorporate and estimate tropospheric delay for both Dry and Wet Mapping function
6	Atmospheric Tidal loading(ATL) and Non-tidal atmospheric loading(ATML)	ftp://everest.mit.edu/pub/GRIDS/	Correction for Tidal and Non-tidal atmospheric loading

Table 2. Basic Processing Parameters

Parameter	Description
RINEX data	30 seconds sampling rate
Orbital Data	IGS final/Precise orbit
Ocean tide loading	FES2004
Ionospheric model	Double difference Ionospheric free(IF) linear combination
Adjustment	Kalman filter
Tropospheric Delay Model	Saastamoinen Model
elevation cut-off	10°
Antenna Model	ELEV
Earth tide model	IERS03
Choice of Experiment	Baseline
Dry and Wet Mapping Function	New Vienna Mapping function (VMF1)
Atmospheric Tidal loading(ATL) and Non-tidal atmospheric loading(ATML)	YES
Observations	30-seconds sampling interval
Satellite Orbits/Earth Orientation Parameters	IGS final orbits(SP3) and IGS final EOP products
A priori Meteorological Observation Source	VMF1

3. Results and Discussions

3.1. *GNSS Precipitable water vapour*

The results of the daily average Precipitable Water Vapour for the years 2012 and 2013 as observed from thirteen (13) NigNet tracking stations namely: ABUZ, BKFP, CGGT, CLBR, FPNO, FUTA, FUTY, GEMB, HUKP, OSGF, RUST, ULAG and UNEC is presented in Figure 2 and Figure 3. From Figure 2, the minimum daily average value of PWV for the year 2012 are 12.41mm, 20.13mm, 28.11mm and 31.63mm for CGGT, GEMB, ABUZ and BKFP respectively.

The maximum average values of PWV were 55.65mm, 54.46mm, 51.27mm and 49.23mm for FPNO, RUST, CLBR and ULAG respectively. Furthermore, from Figure 3, the minimum daily average value of PWV for the year 2013 is 20.36mm, 27.52mm, 30.24mm and 30.56mm for GEMB, ABUZ, HUKP and BKFP respectively, while the maximum daily average values were 56.16mm, 54.43mm, 53.42mm and 48.42mm for RUST, CLBR, FPNO and ULAG respectively. Stations with low PWV (CGGT, GEMB, ABUZ, FUTY and BKFP) fall within the temperate region of the country. While Stations with high PWV (FPNO, RUST, CLBR, UNEC and ULAG) fall within the tropical or coastal region of the country where rainfall is high.

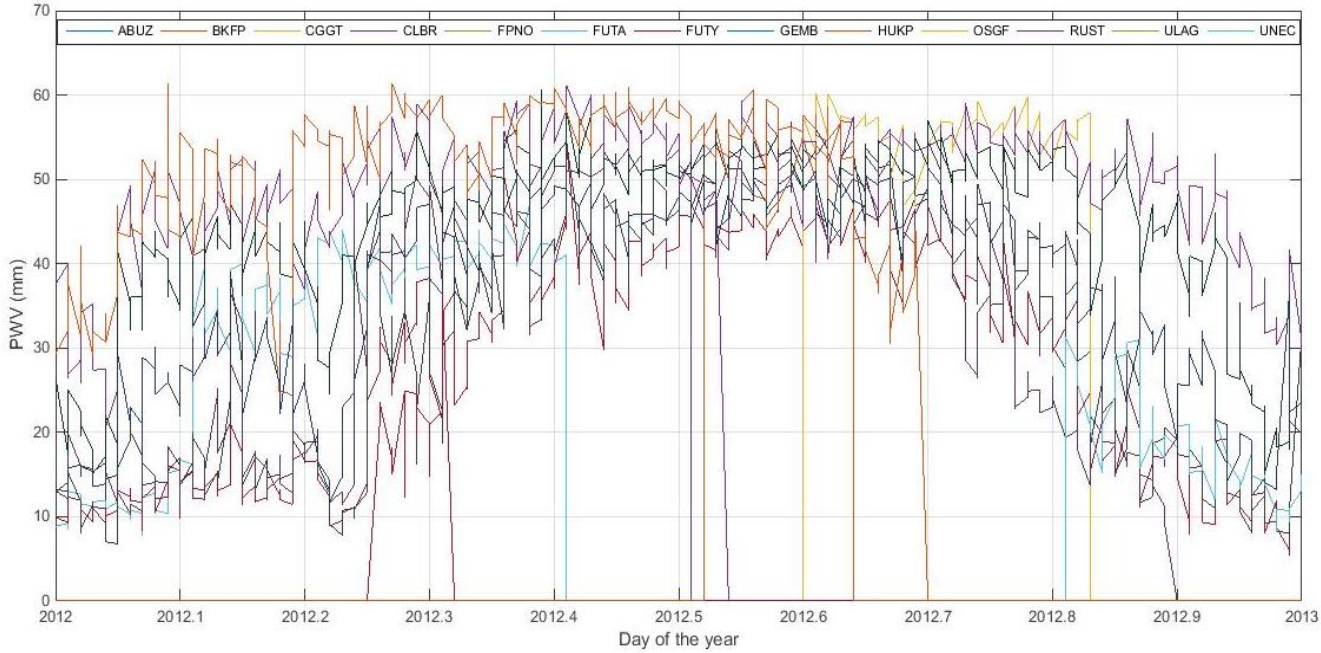

Figure 2. Daily Average PWV from GNSS Observations for Year 2012

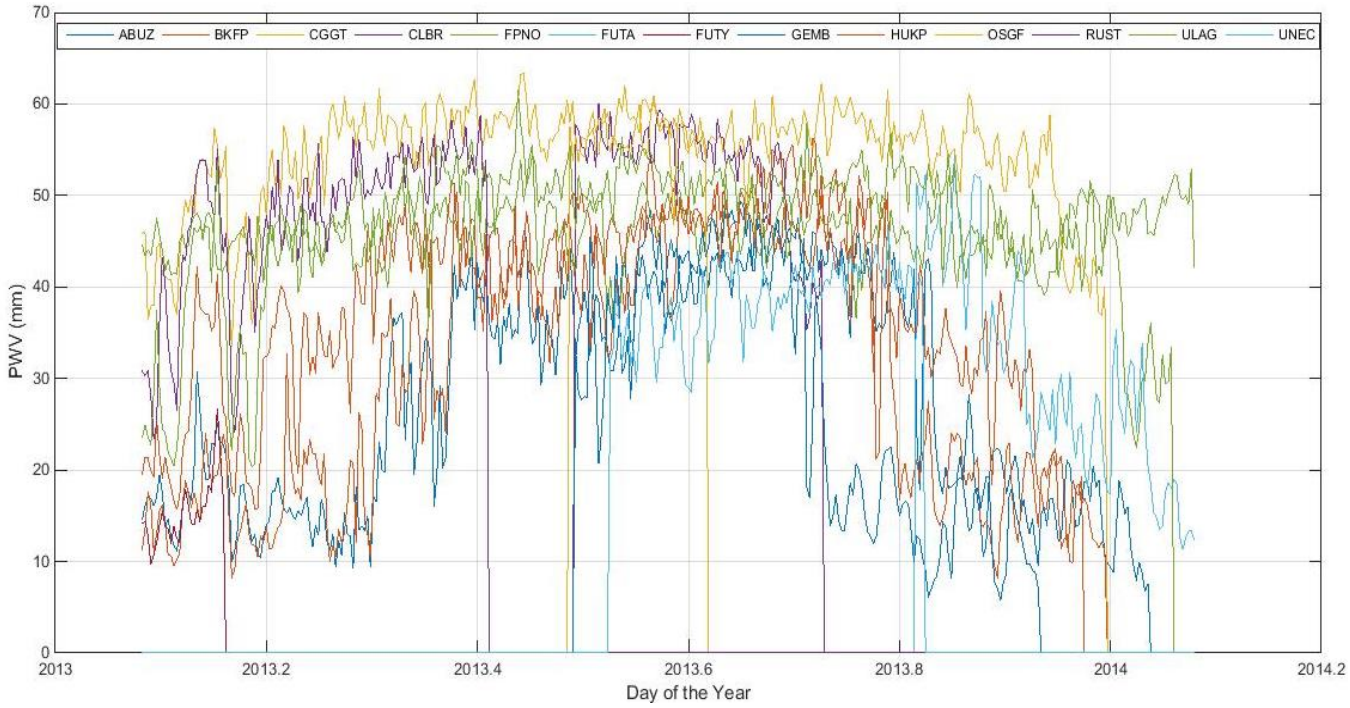

Figure 3. Daily Average PWV from GNSS Observations for Year 2013

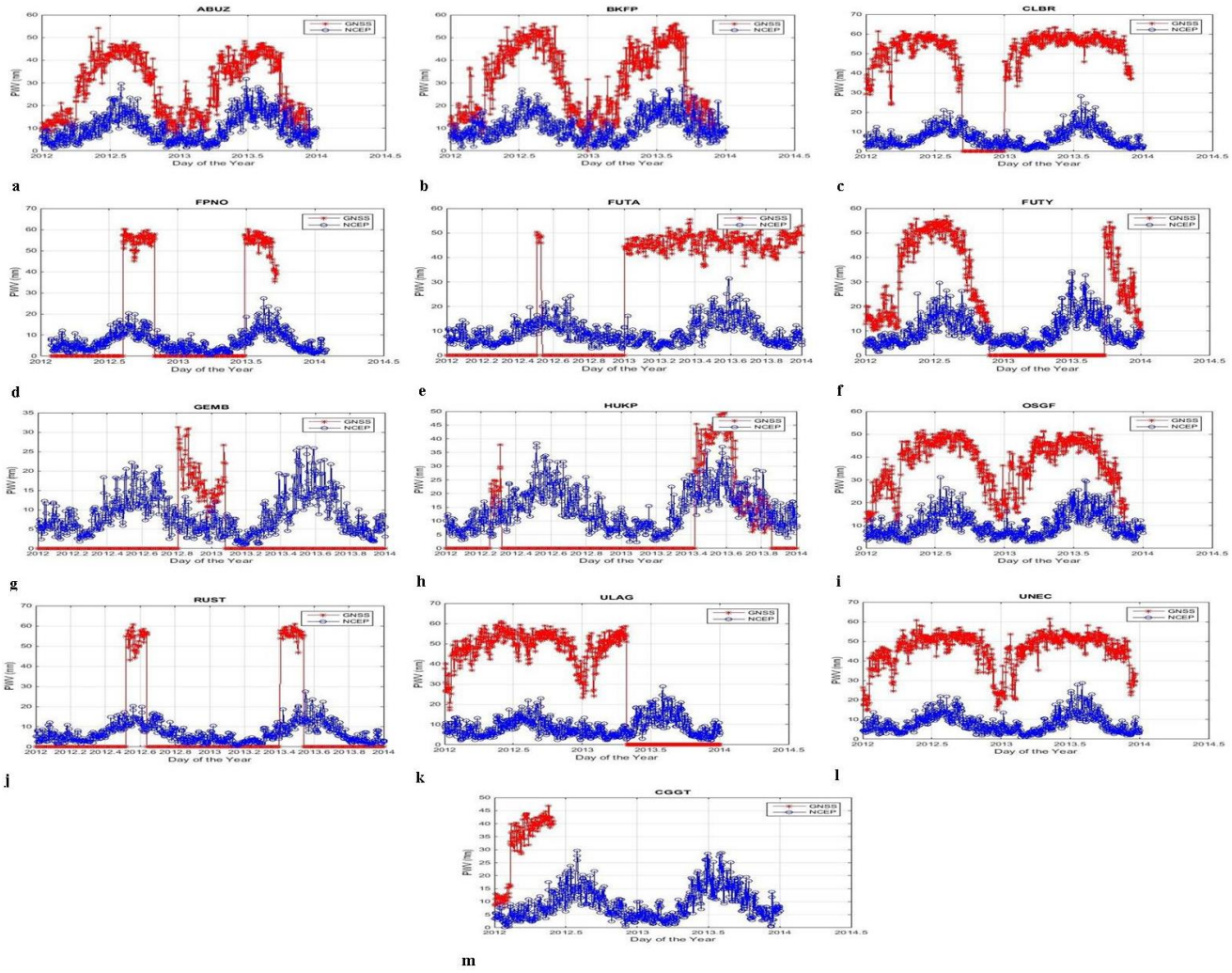

Figure 4. Average Daily PWV for Stations of Interest from GNSS and NCEP for 2012-2013

3.2. Temporal Variability of ground based GNSS PWV and NCEP PWV

The temporal pattern of estimated water vapour from GNSS observation for the study period is compared with NCEP. The temporal correlation of the stations of interest between GNSS and NCEP is presented in Figure 4. Zero values indicate no observation available for such day due to the inconsistencies of the tracking stations. Though, it can be observed that for stations with minimal data gap, the temporal characteristics of the PWV estimated from ground-based GNSS stations is the same for the NCEP PWV.

The coefficient of correlation between the GNSS and NCEP PWV for the thirteen stations namely: ABUZ, BKFP, CGGT, CLBR, FPNO, FUTA, FUTY, GEMB, HUKP, OSGF, RUST, ULAG and UNEC were 0.4541, 0.3312, 0.1728, 0.0076, 0.009, 0.0026, 0.1464, 0.0144, 0.1831, 0.2098, 0.0125, 0.015 and 0.0067 respectively. The results are summarized in Table 3.

Possible reason for weak correlation between GNSS PWV and NCEP PWV as indicated by R2 values in Table 3 is because of the relatively high spatial grid interval (2.50x2.50) of the NCEP, the weighted mean temperature (Tm) adopted and non-collocation of the GNSS stations with Meteorological stations.

Table 3. Summary of Coefficient of Correlation between GNSS and NCEP PWV

S/No	Station ID	R^2	Percentage (%)
1	abuz	0.4541	45.41
2	bkfp	0.3312	33.12
3	cggt	0.1728	17.28
4	clbr	0.0076	0.76
5	fpno	0.009	0.9
6	futa	0.0026	0.26
7	futy	0.1464	14.64
8	gemb	0.0144	1.44
9	hukp	0.1831	18.31
10	osgf	0.2098	20.98
11	rust	0.0125	1.25
12	ulag	0.015	1.5
13	unec	0.0067	0.67

3.3. Validation with Rainfall Events

The GNSS PWV for years 2012 and 2013 are compared with Rainfall events obtained from (http://sdwebx.worldbank.org/climateportal/index.cfm?page=country_history_climate&ThisCCode=NGA) for the years 2012 and 2013 and the results presented in Figure 5 and 6. The monthly PWV increases with monthly rainfall events and vice-versa. This can be observed in Figure 5 and 6.

Seasonally, for year 2012 the PWV is denser in the months of June July, August and September with 51.51mm, 51.56mm and 47.83mm and 50.61mm respectively which are all within the rainy season. On the other hand, the PWV was found to be less in January, February March and December with 21.03mm, 28.34mm, 28.64 and 24.41mm, respectively. This is presented in Figure 5.

Similarly, for year 2013, the PWV is higher in May, June, July and August, with 46.36mm, 48.43mm, 48.24mm and 48.63mm respectively. On the other hand, the PWV was found to be less in, January, February November and December with 28.42mm, 37.72mm, 29.72mm and 20.98mm respectively. The PWV is higher during rainy season and less during dry season. This is presented in Figure 6.

In both Figure 5 and 6 PWV and Rainfall events were found to be high in the months of June, July, August and September and lesser in the months of January, February March and December.

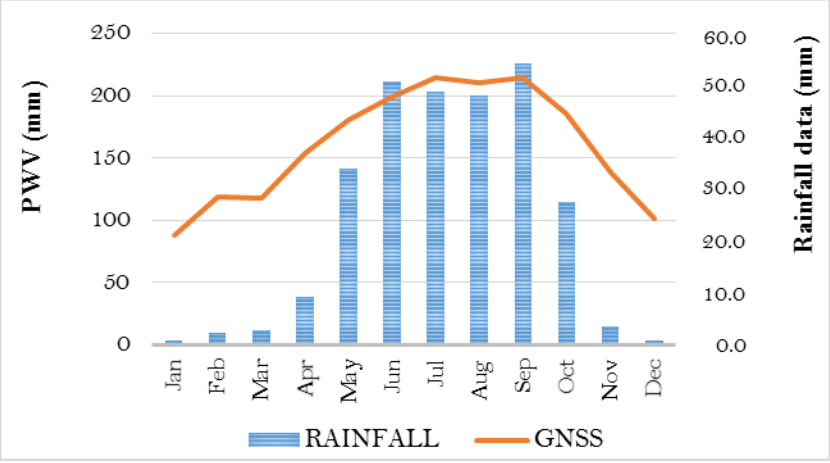

Figure 5. GNSS PWV in Comparison with Rainfall Data for Year 2012

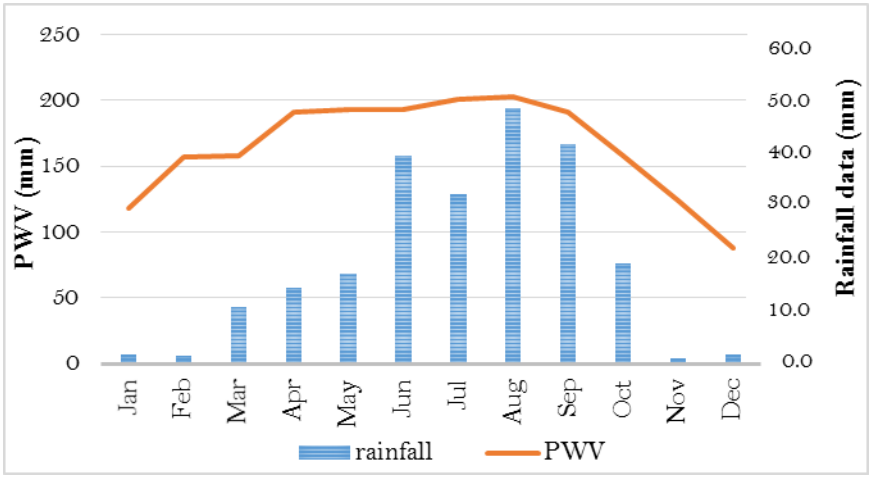

Figure 6. GNSS PWV in Comparison with Rainfall Data for Year 2013

3.4. Spatial Variation of PWV

The Figures 7 and 8 show the spatial variation of PWV across Nigeria for years 2012 and 2013. The PWV for years 2012 and 2013 is high in south-West, South-East South-South part of the country as they are closer to the tropical or coastal region of the country and some parts of North-Central (Kwara, Kogi, Benue and Tarabar) and less in North-East, North-Central and North-West part of the country. The rainfall data is observed to be more in 2012 than 2013 which indicate the 2012 had more rainfall. This clearly justifies that ground-based GNSS stations can be used in climate research and operational weather nowcasting.

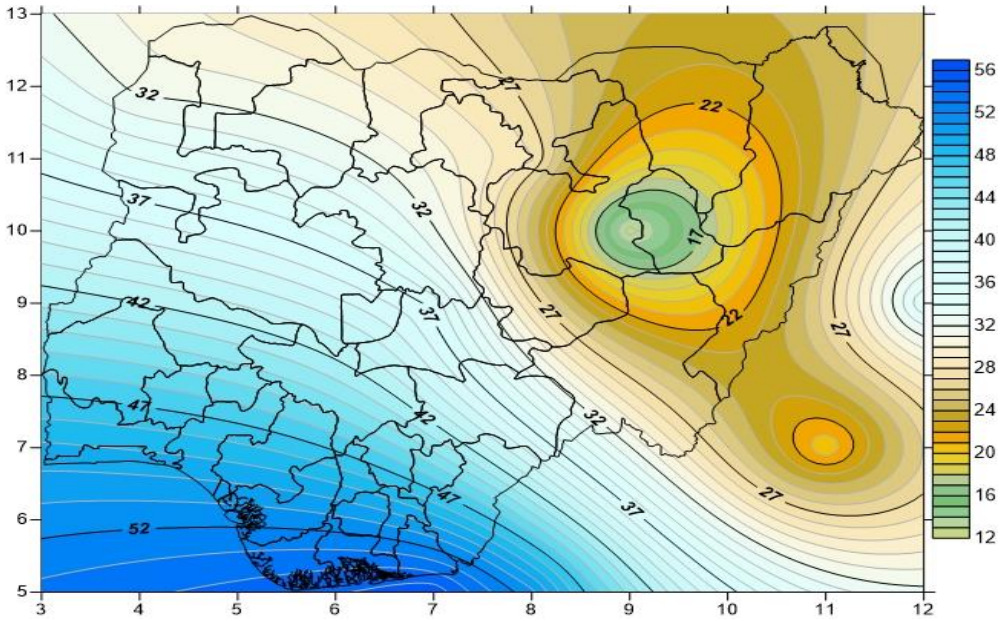

Figures 7. Mean Spatial Distribution of PWV over Nigeria for year 2012

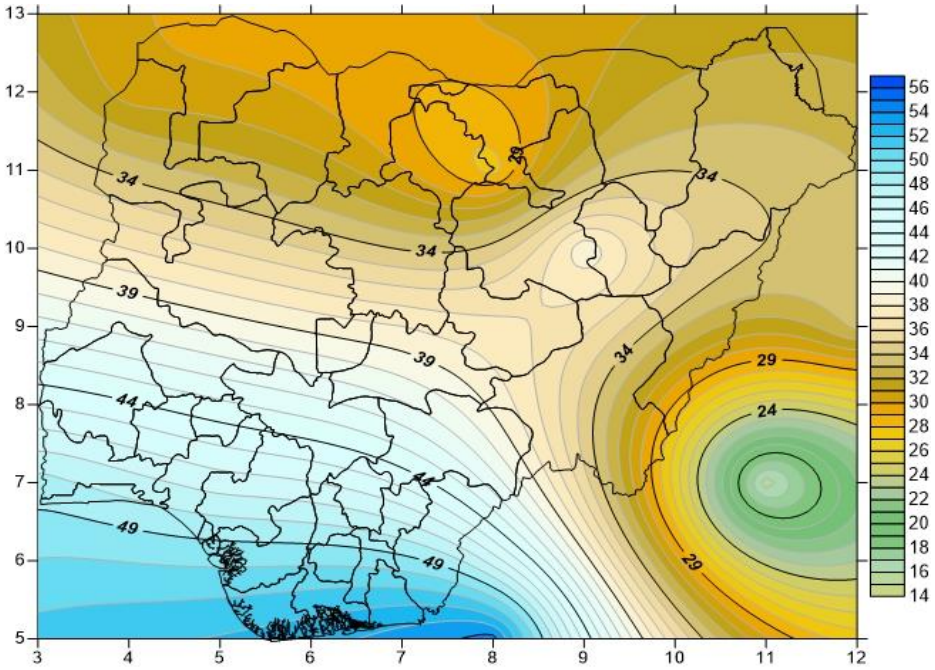

Figure 8. Mean Spatial Distribution of PWV over Nigeria for year 2013

4. Conclusion

The daily average Precipitable Water Vapour for years 2012 and 2013 had been estimated from GNSS observation and the results show that the PWV is more in southern part as the result of their closeness to the coast and attributed to lower elevation. Whereas the PWV was found to be lesser in the Northern part of the country which is attributed to higher elevation. With respect to seasonal variability, it was observed that the PWV is denser in rainy months (April to October) and less in dry season (November to March) due to the fact that the troposphere contains lower amount of water vapour in the winter than in summer. In comparison of GNSS PWV with Rainfall data and NCEP PWV for 2012 and 2013, a good correlation was observed both spatially and temporally with respect to rainfall data. As for the NCEP PWV, the coefficient of determination of R2 was observed to be more in Northern part and less in southern part of the country which indicate weak correlation between the two. It is therefore concluded that GNSS can be used in numerical weather assimilation and operational weather now casting.

5. Acknowledgement

The authors would like to express their profound gratitude to the Office of the Surveyor General of the Federation (OSGOF) for the GNSS data. Massachusetts Institute of Technology (MIT) is also appreciated for making GAMIT/GLOBK a freeware.

6. References

Bawa, S., Ojigi, L. M., & Dodo, J. D. (2017). GPS velocity time series of NigNET CORS. *Nigeria Association of Geodesy (NAG) General Assembly/Scientific Conference Rivers State University, Port-Harcourt, Nigeria*, 24–27.

Bevis, M., Businger, S., Chiswell, S., Herring, T. A., Anthes, R. A., Rocken, C., & Ware, R. H. (1994). GPS Meteorology: Mapping Zenith Wet Delays onto Precipitable Water. *Journal of Applied Meteorology*, *33*(3), 379–386. [Crossref]

Bevis, M., Businger, S., Herring, T. A., Rocken, C., Anthes, R. A., & Ware, R. H. (1992). GPS Meteorology: Remote sensing of atmospheric water vapor using the global positioning system. *Journal of Geophysical Research*, *97*(D14), 15787. [Crossref]

Boutiouta, S., & Lahcene, A. (2013). Preliminary study of GNSS meteorology techniques in Algeria. *International Journal of Remote Sensing*, *34*(14), 5105–5118.

Chen, B., & Liu, Z. (2015). A comprehensive evaluation and analysis of the performance of multiple tropospheric models in China region. *IEEE Transactions on Geoscience and Remote Sensing*, *54*(2), 663–678.

Davis, J. L., Herring, T. A., Shapiro, I. I., Rogers, A. E. E., & Elgered, G. (1985). Geodesy by radio interferometry: Effects of atmospheric modeling errors on estimates of baseline length. *Radio Science*, *20*(6), 1593–1607. [Crossref]

Godah, W., Szelachowska, M., Ray, J. D., & Krynski, J. (2020). Comparison Of Vertical Deformations Of The Earth's Surface Obtained Using Grace-Based GGMS And GNSS Data--A Case Study Of South-Eastern Poland. *Acta Geodyn. Geomater*, *17*, 169–176.

Gurbuz, G., Jin, S., & Mekik, C. (2015). Sensing Precipitable Water Vapor (PWV) using GPS in Turkey - Validation and Variations. In *Satellite Positioning - Methods, Models and Applications*. [Crossref]

Herring, T. A., King, R. W., & McClusky, S. C. (2010). *Introduction to GAMIT/GLOBK*.

Isioye, O. A., Combrinck, L., & Botai, J. (2016). Modelling weighted mean temperature in the West African region: implications for GNSS meteorology. *Meteorological Applications*, *23*(4), 614–632. [Crossref]

Kindu, T. A. (2017). *Tectonics And Crustal Deformation In Ethiopia From Continuously Operating Reference Stations*.

Li, Y. (2021). Analysis of GAMIT/GLOBK in high-precision GNSS data processing for crustal deformation. *Earthquake Research Advances*, *1*(3), 100028. [Crossref]

Liu, J., Chen, X., Sun, J., & Liu, Q. (2017). An analysis of GPT2/GPT2w+ Saastamoinen models for estimating zenith tropospheric delay over Asian area. *Advances in Space Research*, *59*(3), 824–832.

Perevalova, N. P., Romanova, E. B., & Tashchilin, A. V. (2020). Detection of high-latitude ionospheric structures using GNSS. *Journal of Atmospheric and Solar-Terrestrial Physics*, *207*, 105335. [Crossref]

Saastamoinen, J. (1972). Atmospheric correction for the troposphere and stratosphere in radio ranging satellites. *The Use of Artificial Satellites for Geodesy*, *15*, 247–251.

Suresh Raju, C., Saha, K., Thampi, B. V, & Parameswaran, K. (2007). Empirical model for mean temperature for Indian zone and estimation of precipitable water vapor from ground based GPS measurements. *Annales Geophysicae*, *25*(9), 1935–1948.

Tregoning, P., Boers, R., O'Brien, D., & Hendy, M. (1998). Accuracy of absolute precipitable water vapor estimates from GPS observations. *Journal of Geophysical Research: Atmospheres*, *103*(D22), 28701–28710. [Crossref]

Tsai, M.-C., Yu, S.-B., Shin, T.-C., Kuo, K.-W., Leu, P.-L., Chang, C.-H., & Ho, M.-Y. (2015). Velocity Field Derived from Taiwan Continuous GPS Array (2007-2013). *Terrestrial, Atmospheric & Oceanic Sciences*, *26*(5).

Tsidu, G. M., Blumenstock, T., & Hase, F. (2015). Observations of precipitable water vapour over complex topography of Ethiopia from ground-based {GPS}, {FTIR}, radiosonde and {ERA}-Interim reanalysis. *Atmospheric Measurement Techniques*, *8*(8), 3277–3295. [Crossref]

Uang-Aree, P., Kingpaiboon, S., & Khuanmar, K. (2014). Estimation of missing GPS precipitable water vapor data by zenith wet delay and meteorological data. *Advanced Materials Research*, *931*, 703–708.

Wielgosz Paweł and Hadaś, T., Kłos, A., & Paziewski, J. (2019). Research on GNSS positioning and applications in Poland in 2015--2018. *Geodesy and Cartography*, 87–119.

Xiaoming, L., Lisheng, X., Yansong, F., Yujie, Z., Jilie, D., Hailei, L., & Xiaobo, D. (2010). Estimation of the Precipitable Water Vapor from ground-based GPS with GAMIT/GLOBK. *2010 Second IITA International Conference on Geoscience and Remote Sensing*. [Crossref]